

Sputtering of Tetrafluoro- and Tetraphenylborate Anions Adsorbed to an Amine-Terminated Self-Assembled Monolayer Surface

Michael J. Van Stipdonk,* Robert D. English, and Emile A. Schweikert

Department of Chemistry, P.O. Box 30012, Texas A&M University, College Station, Texas 77843-3012

Received: May 24, 1999

Secondary ion mass spectrometry was used to monitor the exchange of tetrafluoro- and tetraphenylborate anions to the surface of an amine-terminated self-assembled monolayer. The exchanged surfaces were prepared by soaking aminoethanethiol (AET) monolayers on Au in solutions of the respective sodium salts. The mass spectra produced from the monolayer surface and those from Au blank and propanethiol monolayers soaked in the same salt solutions demonstrate that the protonated amine terminus of the AET monolayer is important to the uptake of the inorganic anion. The exchanged monolayer surfaces were used to measure secondary ion yields produced from ultrathin films by $(\text{CsI})_n\text{Cs}^+$ ($n = 0-2$) projectiles at the limit of single-ion impacts. The yield trends produced from the monolayer surface as a function of projectile complexity and energy differ dramatically from those generated from thicker targets of solid NaBF_4 and NaB(Ph)_4 . Nonlinear enhancements (expressed as an increase in the secondary ion yield per projectile atom) in the yield of BF_4^- and B(Ph)_4^- are observed for the polyatomic ion impacts on the thick targets. For the yields of the same anions sputtered from the exchanged monolayer, however, a slight nonlinear enhancement was observed only for the $(\text{CsI})\text{Cs}^+$ projectile, and the enhancement is greatly reduced compared to the thick target.

Introduction

In secondary ion mass spectrometry (SIMS), polyatomic or molecular primary ions are known to produce enhanced secondary ion yields when compared to atomic primary ions at similar impact energy and velocity.¹⁻¹⁰ A yield enhancement may be defined either as an increase in secondary ion yield *per projectile constituent*³ or as an increase in the secondary ion yield *per unit surface damage*.⁹ To date, most comparative studies of atomic and polyatomic ion-induced sputtering have employed thick organic and inorganic targets. Recently, the enhancement of ion yields from thin film and monolayer targets has also been investigated.¹¹⁻¹³ Yield enhancements of 10–100 times have been reported for polyatomic projectile impacts on thick (multilayer) targets such as amino acids and polymers. The enhancements are either greatly reduced or not observed when atomic and polyatomic projectile impacts on ultrathin targets such as Langmuir–Blodgett films¹² or self-assembled monolayers (SAM) are compared.¹³

SAMs provide interesting targets for studying desorption phenomena induced by monatomic and polyatomic projectile impacts. *n*-Alkanethiol monolayers on Au spontaneously form densely packed, two-dimensional surface assemblies via Au–S bonds.¹⁴ The thickness, order, and surface properties of the monolayer can be selected by changing the chain length, composition, or terminal functional group. For instance, AET monolayers feature an amine terminus that is protonated at neutral pH. AET monolayer surfaces have been used to adsorb nucleotides and oligonucleotides for subsequent analysis by SIMS¹⁵ and have also been used to desalt analyte solutions by ion-pair formation during sample preparation for matrix-assisted laser desorption/ionization mass spectrometry.¹⁶

The objectives of the experiments reported here were (a) to determine whether the protonated AET surface will adsorb complex inorganic ions by anion exchange and (b) to use the

anion exchange properties to prepare thin films for sputter yield measurements using polyatomic primary ions. The former consideration is important to studies of the controlled growth of inorganic materials on monolayer surfaces, while the latter will contribute to the present understanding of polyatomic ion impacts on ultrathin films. In this paper we demonstrate the uptake of tetrafluoroborate $[\text{BF}_4^-]$ and tetraphenylborate $[\text{B(Ph)}_4^-]$ anions from aqueous solution by AET monolayers. In addition, the relative yields of BF_4^- and B(Ph)_4^- from the exchanged monolayers generated by Cs^+ , $(\text{CsI})\text{Cs}^+$, and $(\text{CsI})_2\text{Cs}^+$ projectile impacts were measured at incident energies ranging from 10 to 26 keV. The relative ion yields obtained from the exchanged monolayers are also compared to those generated from thick solid targets of the respective sodium salts.

Experimental Section

Materials. Si wafers (4 in., PB100) were purchased from Wafer World, Inc. (W. Palm Beach, FL). The wafers were coated with a 10 nm Ti adhesion layer followed by a 200 nm thick Au layer (Lance Goddard Associates, Forest City, CA). Propanethiol, sodium tetrafluoroborate, and sodium tetraphenylborate were purchased from Aldrich and used as received. Aminoethanethiol was a gift from R. M. Crooks at Texas A&M University. Ethanol was purchased from AAPER Alcohol and Chemical Co. (Shelbyville, KY) and used as received.

Monolayer Preparation. The Au-coated Si wafers were cut into 1 cm² pieces using a diamond scribe, rinsed with ethanol, and ozone cleaned for 10 min under UV light. To prepare SAM surfaces, the Au–Si substrates were immersed in 1 mM ethanolic solutions of either AET or propane thiol and left to soak for 18 h. The monolayer-coated substrates, once removed from the thiol solution, were rinsed with 0.1 M HCl to ensure protonation of the terminal amine and transferred immediately to a vial containing 3 mM solutions of sodium tetrafluoro- or

tetraphenylborate. The monolayer samples were soaked in salt solution for 1 h. The monolayer samples were then removed, and the excess solution was carefully drawn off by allowing it to soak into the edge of a paper towel. We found that drying the exchanged monolayers with a stream of dry nitrogen caused rapid evaporation of the excess solution to produce multilayers of salt by precipitation. The wafers were then quickly mounted to the sample support for the mass spectrometer using double-sided tape.

Thick Target Preparation. Ion yield measurements were also conducted using solid NaBF_4 and NaB(Ph)_4 . In contrast to the exchanged monolayer samples, these targets can be considered infinitely thick relative to the range and penetration of the primary ion (ca. 10–100 nm). To prepare thick samples, 0.3 M solutions of NaBF_4 and NaB(Ph)_4 were prepared in distilled/deionized (DI) water. A 10 μL aliquot of solution was applied to a roughened stainless steel sample support (1.5×2 cm) and allowed to dry at room temperature in a dark fume hood. The solution concentration was chosen empirically to produce thin, homogeneous coverage of the sample support with minimal caking and crust formation. The sample supports were then inserted into the mass spectrometer for analysis.

Mass Spectrometry. Negative ion mass spectra were collected using a custom dual time-of-flight (ToF) SIMS instrument. The configuration and operation of the instrument have been described in detail elsewhere.¹ Cs^+ , $(\text{CsI})\text{Cs}^+$, and $(\text{CsI})_2\text{Cs}^+$ primary ions with incident energies ranging from 10 to 26 keV were used to bombard the monolayer and thick target surfaces at an impact angle of 27° . These experiments were performed using event-by-event bombardment/detection and a coincidence counting protocol. This method allowed the measurement of secondary ion yields at the limit of single projectile impacts.

Secondary electron emission from the sample target was used to measure the number of incident primary ions. Relative secondary ion yields were calculated by dividing the integrated peak area of a particular secondary ion by the number of incident primary ions. The relative ion yields are thus a measure of the number of secondary ions detected per incident primary ion without correction for instrument transmission and detection efficiency. The event-by-event bombardment and detection mode and coincidence protocol used in these experiments allowed the atomic and polyatomic projectiles to be compared simultaneously under the same experimental conditions.^{1,3}

Studies on the use of SIMS to characterize SAM surfaces have demonstrated that the yields of intact, molecularly specific peaks (e.g., thiolate or Au–thiolate species) from atomic and polyatomic ion impacts are low.^{13,17} Conversion of the thiolate to a sulfonate via UV oxidation is known to improve the yield of secondary ions specific to monolayer surfaces.¹³ In the present study, the presence of AET and propanethiol monolayers on the Au substrate was confirmed by collecting a mass spectrum from monolayers oxidized using UV light under ambient conditions.¹⁸

Results and Discussion

Anion Exchange. Figure 1 shows two negative ion mass spectra collected from the same AET monolayer sample. The first (Figure 1a) was collected from the AET surface following a rinse with 0.1 M HCl. The second (Figure 1b) was collected from the same monolayer following a soak in 3 mM NaBF_4 for 1 h. The spectra were acquired using 20 keV Cs^+ primary projectiles at a dose of ca. 10^6 ions/ cm^2 . Aside from the background peaks (<30 amu) common to all samples run in

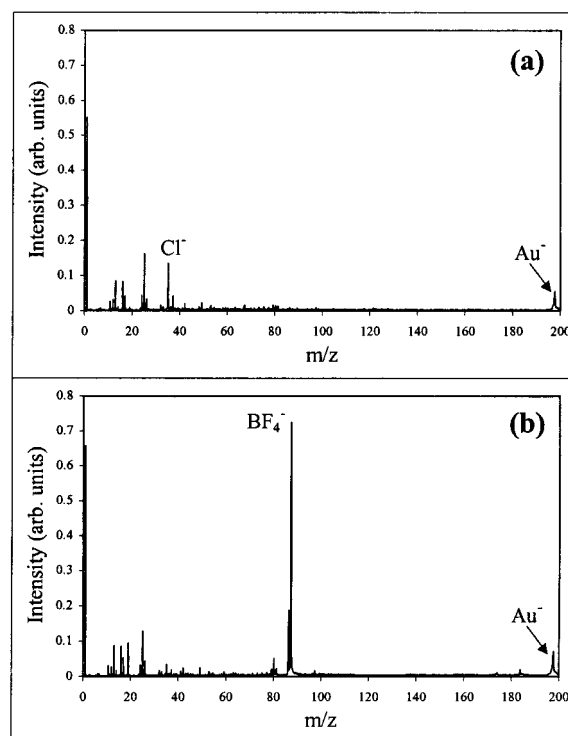


Figure 1. Negative secondary ion mass spectra of an aminoethane thiol monolayer on Au: (a) following rinse with 0.1 M HCl and (b) following immersion in 3 mM aqueous NaBF_4 . The spectra were acquired using 20 keV Cs^+ projectiles at a dose of $\sim 10^6$ ions/ cm^2 . The ion intensities in both spectra are corrected for the number of incident primary ions.

the SIMS instrument, the most prominent features in Figure 1a are ions at mass-to-charge ratio (m/z) 35 and 37, representing Cl^- presumably adsorbed to the protonated amine during the HCl rinse. In Figure 1b, a prominent peak at m/z 87 (with the associated ^{10}B isotope peak at m/z 86) indicates the uptake and ion exchange (for Cl^-) of BF_4^- by the AET monolayer. Qualitatively similar spectra were collected from the same surfaces using $(\text{CsI})\text{Cs}^+$ and $(\text{CsI})_2\text{Cs}^+$ primary projectiles at doses of ca. 10^5 and 10^4 ions/ cm^2 , respectively. Figure 2 shows the negative ion mass spectrum of a second AET monolayer following a rinse with 0.1 M HCl (Figure 2a) and following a subsequent soak in 3 mM NaB(Ph)_4 for 1 h (Figure 2b). The uptake of B(Ph)_4^- by the AET monolayer is clearly demonstrated by the appearance of the prominent peak characteristic of the intact anion at m/z 319. Qualitatively similar spectra were produced by $(\text{CsI})\text{Cs}$ and $(\text{CsI})_2\text{Cs}$ primary ions.

The BF_4^- and B(Ph)_4^- -exchanged AET monolayers were removed from the instrument and rinsed with 1 mL of DI water. The B(Ph)_4^- -exchanged monolayer exhibited a strongly hydrophobic character and was not wet by the rinse solution. Both samples were then reinserted into the mass spectrometer. Subsequent mass spectra indicated that the BF_4^- was removed from the monolayer by the rinse step. A significant amount of B(Ph)_4^- remained after the rinse. Using new wafers in a separate set of experiments, AET monolayers exchanged with BF_4^- and B(Ph)_4^- were soaked for 30 s in 0.1 M HCl. Mass spectra of samples collected after the HCl soak indicated that the BF_4^- and B(Ph)_4^- was largely replaced by Cl^- .

To determine the importance of the protonated amine terminus on the uptake of BF_4^- by the AET monolayer, a blank (Au-coated Si wafer without AET monolayer) and a propanethiol monolayer sample were immersed in the same 3 mM NaBF_4 solution and soaked for 1 h. The propanethiol monolayer served

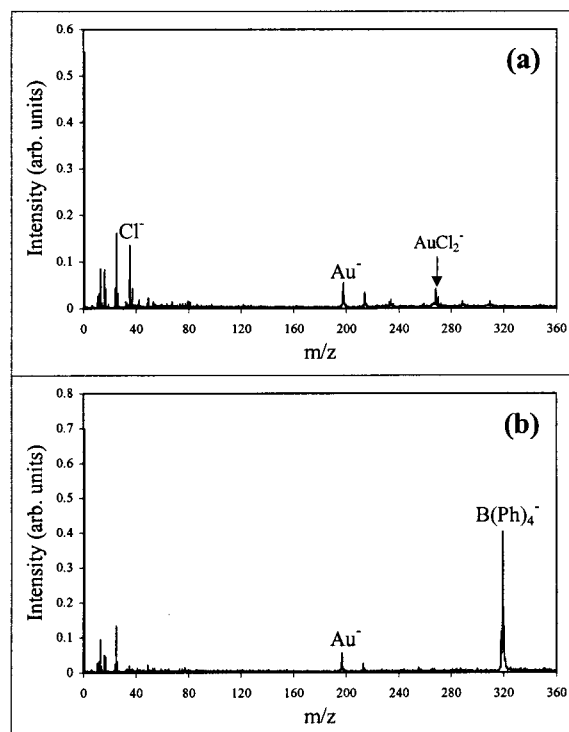


Figure 2. Negative secondary ion mass spectra of an aminoethane thiol monolayer on Au: (a) following rinse with 0.1 M HCl and (b) following immersion in 3 mM aqueous NaB(Ph)₄. The spectra were acquired using 20 keV Cs⁺ projectiles at a dose of $\sim 10^6$ ions/cm². The ion intensities in both spectra are corrected for the number of incident primary ions.

as a methyl-terminated analogue to the AET monolayer. Secondary ion peaks at m/z 86 or 87 (BF₄[−]) were not observed in the ToF-SIMS spectra of the Au-Si blank. A weak BF₄[−] peak was observed in the spectrum produced from the propanethiol monolayer. The intensity of the BF₄[−] peak was reduced by a factor of 10, however, relative to the AET monolayer.

Figure 3 shows the mass spectra produced by 20 keV Cs⁺ projectile impacts on thick samples (see Experimental Section) of NaBF₄ and NaB(Ph)₄. The relative yields measured for several secondary ions sputtered by 20 keV Cs⁺, (CsI)Cs⁺, and (CsI)₂Cs⁺ impacts on the exchanged monolayer and thick sample targets are listed in Table 1. Several noteworthy observations were made. The mass spectrum produced by 20 keV Cs⁺ impacts on the NaBF₄ (thick) target, in agreement with earlier studies,¹⁹ is dominated by the F[−] ion at m/z 19. Less intense peaks characteristic of NaBF₄ such as BF₄[−] and (NaBF₄)BF₄[−] (m/z 195, 196, 197) were also observed. The latter ion exhibits a characteristic triplet pattern due to the ¹⁰B and ¹¹B isotopes and was not observed in the mass spectrum collected from the AET monolayer exchanged with BF₄[−]. An isobaric ion at m/z = 197 was observed in the exchanged monolayer spectrum and is attributed to Au[−]. In contrast to the NaBF₄ target, the spectrum produced by 20 keV Cs⁺ impacts on the exchanged monolayer surface is dominated by the BF₄[−] ion, and intensity of the F[−] peak is dramatically reduced. The differences between the solid target and the exchanged monolayer in terms of the relative yields of F[−] and BF₄[−], and the lack of a (NaBF₄)BF₄[−] ion in the mass spectrum of the exchanged surface, support the conclusion that ion exchange results in submonolayer to monolayer coverage of BF₄[−] on the AET/Au surface.

The relative ion yields produced from the various target surfaces by the (CsI)_nCs⁺ projectiles can be compared with the

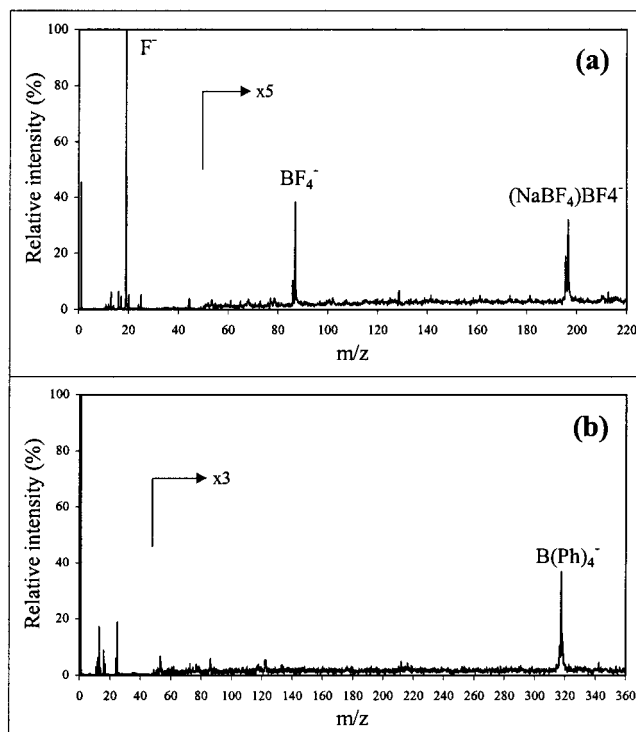


Figure 3. Negative secondary ion mass spectra collected from thick target samples of (a) NaBF₄ and (b) NaB(Ph)₄. The sample targets were prepared as described in the text. Primary projectiles: 20 keV Cs⁺ at doses of $\sim 10^6$ (a) and 10^7 (b) ions/cm².

TABLE 1: Relative Yields of Selected Secondary Ions Sputtered from Exchanged Monolayer and Thick Target Samples by 20 keV Cs, (CsI)Cs, and (CsI)₂Cs Primary Ions^a

secondary ion	primary projectile (20 keV)		
	Cs ⁺	(CsI)Cs ⁺	(CsI) ₂ Cs ⁺
exchanged targets			
F [−]	0.7 (±0.007)	0.91 (±0.008)	1.1 (±0.01)
BF ₄ [−]	4.4 (±0.04)	8.5 (±0.07)	9.2 (±0.09)
B(Ph) ₄ [−]	3.1 (±0.03)	4.0 (±0.04)	4.2 (±0.04)
thick targets			
F [−]	2.4 (±0.03)	3.2 (±0.03)	3.6 (±0.04)
BF ₄ [−]	0.15 (±0.002)	8.1 (±0.09)	16.0 (±0.2)
B(Ph) ₄ [−]	0.24 (±0.003)	2.6 (±0.03)	3.0 (±0.03)

^a Using the procedure described in the experimental section, the yields were obtained from three independent experimental runs on the same target surface and the value in parentheses is the relative standard deviation

caveat that the amount of BF₄[−] and B(Ph)₄[−] present on the exchanged monolayers is lower than in the thick targets. In general, for a given secondary ion, the relative yield increase with respect to the mass and complexity of the primary ion is greater for projectile impacts on the thick targets. For instance, the yield of BF₄[−] using (CsI)₂Cs⁺ over Cs⁺ increases by a factor of 2 for the exchanged monolayer and a factor of 100 for the thick target. The exception is the yield of F[−], which shows a yield increase of ~ 1.5 from both sample targets. Previous measurements of ion yields following polyatomic projectile impact have demonstrated that increases in yield are largest for polyatomic secondary ions.^{1,3} The yield of atomic secondary ions, such as F[−] in the present case, is often improved by only a factor of 2–3. We attribute this to the fact that atomic secondary ions are most likely sputtered by the intersection of single recoil cascades with the surface, a condition easily generated by atomic projectile impacts. In contrast, the overlap of multiple localized recoil cascades, acting in concert, is

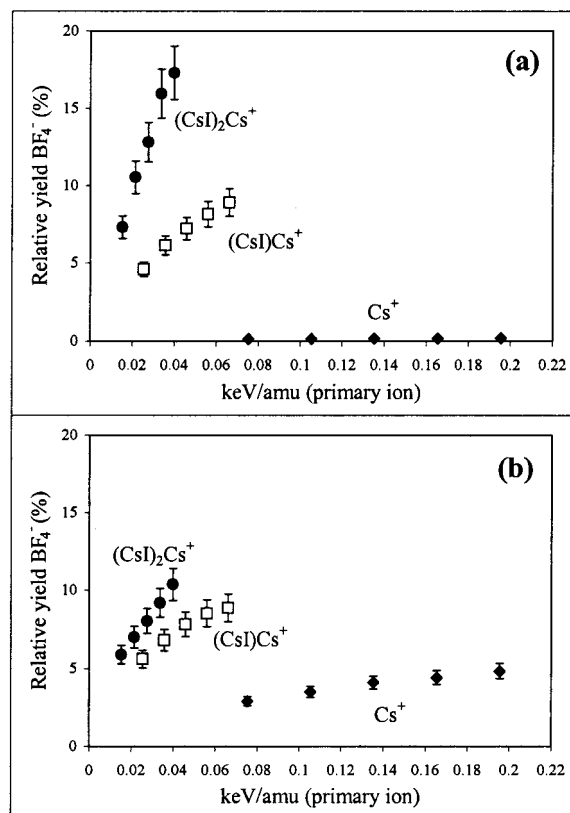


Figure 4. Relative yield of BF_4^- sputtered from (a) solid NaBF_4 and (b) BF_4^- -exchanged AET monolayer surfaces by Cs^+ , $(\text{CsI})\text{Cs}^+$, and $(\text{CsI})_2\text{Cs}^+$ projectiles at impact energies ranging from 10 to 25 keV. The yields are plotted as a function of primary ion energy per mass unit, which is proportional to the square of the projectile velocity.

necessary to sputter polyatomic secondary ions (see discussion below): the probability for generating overlapping cascades is higher following a polyatomic projectile impact. Thus the lack of a significant increase in the yield of F^- by polyatomic ion impacts is due to the relatively high efficiency for generating this secondary ion by atomic ion impacts.

Secondary Ion Yield Measurements at Different Primary Ion Impact Energies. Nonlinear enhancements in secondary ion yield, with respect to the number of atoms in the impacting ion, have been reported in sputtering experiments using Au_n^{+3} and $(\text{CsI})_n\text{Cs}^+$ projectiles.²⁰ A nonlinear enhancement with respect to the projectile complexity exists when the secondary ion yield *per projectile atom* produced by a cluster projectile composed of n constituents is greater than the sum of the yields produced by the individual impact of n atomic projectiles.³ The projectile comparisons are made at the same incident energy per atom (proportional to the incident velocity). The yield enhancements are attributed to the high energy density deposited into a given volume of the solid by polyatomic projectiles. This is due to the overlap of collision cascades initiated by the individual projectile constituents.^{19,21,22}

To determine whether polyatomic primary ions produce yield enhancements from the exchanged monolayer surfaces, Cs^+ , $(\text{CsI})\text{Cs}^+$, and $(\text{CsI})_2\text{Cs}^+$ were used to bombard the BF_4^- -exchanged and $\text{B}(\text{Ph})_4$ -exchanged monolayers and the NaBF_4 and $\text{NaB}(\text{Ph})_4$ targets at incident energies ranging from 10 to 26 keV. Figure 4 shows the relative yield of BF_4^- measured from projectile impacts on (a) solid NaBF_4 and (b) BF_4^- -adsorbed to an AET monolayer. The yields are plotted as a function of the kinetic energy (keV) per atomic mass unit (amu), which is proportional to the square of the projectile velocity.

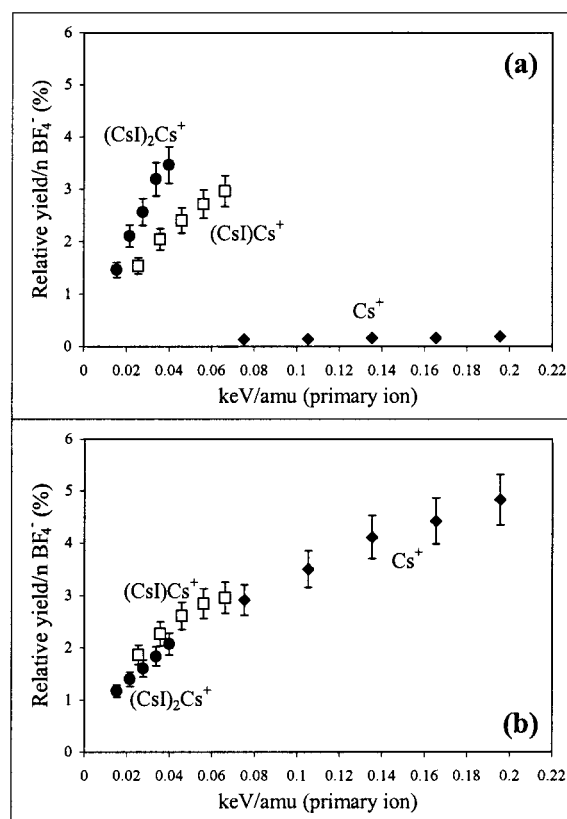


Figure 5. Relative yield of BF_4^- per impacting projectile atom, sputtered from (a) solid NaBF_4 and (b) BF_4^- -exchanged AET monolayer surfaces by Cs^+ , $(\text{CsI})\text{Cs}^+$, and $(\text{CsI})_2\text{Cs}^+$ projectiles at impact energies ranging from 10 to 25 keV. The yields per incident atom are plotted as a function of primary ion energy per mass unit, which is proportional to the square of the projectile velocity.

In both Figure 4a,b, it is clear that higher relative secondary ion yields are produced by the polyatomic primary ions, in agreement with previous studies of polyatomic ion induced sputtering.^{1-3,19-21}

In Figure 5, the relative yields of BF_4^- are divided by the number of projectile atoms and plotted again versus the kinetic energy per mass unit of the primary ion. Because the yields per atom are being compared at the same incident energy per atom, the influence of the number of projectile atoms on secondary ion yield is measured directly. Due to limitations to the primary ion kinetic energies accessible in the current instrument configuration, the Cs^+ and $(\text{CsI})_n\text{Cs}^+$ projectiles could not be compared at the same incident velocity. At impact energies below 10 keV the fixed acceleration potential on the target substrate causes considerable deflection of the primary ion trajectory and impact angle of incidence. Secondary ion yields scale with $1/\cos^2 \theta$, where θ is the angle of incidence. Sufficient overlap in impact energy per atom was possible for the two polyatomic projectiles. Assuming that the measured relative yields produced by Cs^+ continue a linear trend to lower velocities, it is clear from Figure 5a that the relative yield of BF_4^- from the NaBF_4 target *per projectile constituent* (relative yield/ n) increases as the projectile complexity increases from 1 to 5 atoms. A different trend, however, was observed for sputtering from the BF_4^- -exchanged monolayer. In this case, the relative yield/ n of BF_4^- increases with the velocity of the primary ion, but not as sharply with the number of projectile atoms. Within the error of our measurements ($\pm 10\%$ RSD) there is a slight increase in the yield of BF_4^- produced by the $(\text{CsI})\text{-Cs}$ projectile over Cs^+ and $(\text{CsI})_2\text{Cs}^+$. A more accurate

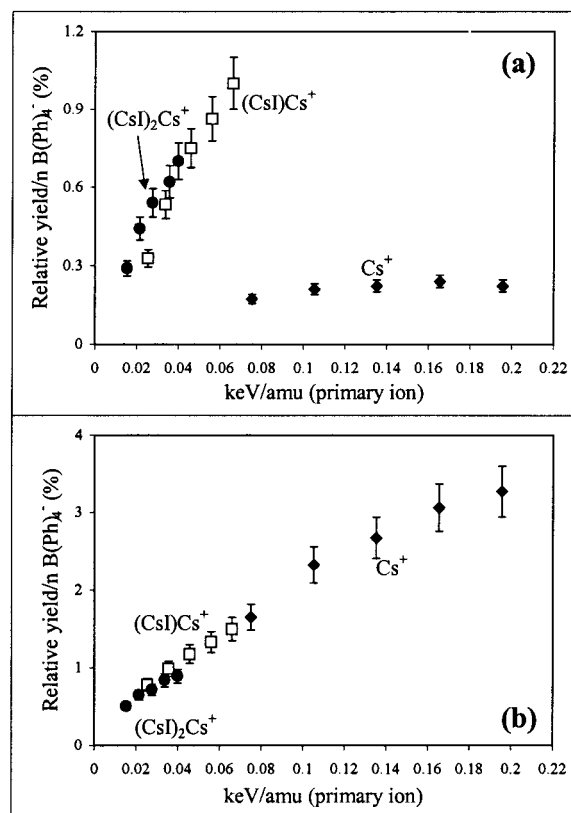


Figure 6. Relative yield of B(Ph)_4^- per impacting projectile atom, sputtered from (a) solid NaB(Ph)_4 and (b) B(Ph)_4^- -exchanged AET monolayer surfaces by Cs^+ , $(\text{CsI})\text{Cs}^+$, and $(\text{CsI})_2\text{Cs}^+$ projectiles at impact energies ranging from 10 to 25 keV. The yields per incident atom are plotted as a function of primary ion energy per mass unit, which is proportional to the square of the projectile velocity.

measurement of the nonlinear yield increase from the exchanged sample requires better overlap of the projectile velocities. It is clear, however, that the yield trends produced from the thick and exchanged targets differ significantly. Figure 6 shows that qualitatively similar trends were produced using the relative ion yields from the solid NaB(Ph)_4 and B(Ph)_4^- -exchanged AET monolayer samples.

The solid samples and the AET monolayers exchanged with BF_4^- and B(Ph)_4^- exhibit different trends in ion yield *per projectile constituent* when measured as a function of incident ion velocity. The pronounced difference may be due to the unique nature of the exchanged monolayer surface. The yield enhancements created by polyatomic ion impacts are attributed to the high energy density or the number of overlapping recoil cascades generated in a given volume of the solid. Multiple recoil cascades generated by polyatomic projectiles are predicted to act "cooperatively" to increase the number of recoil target atoms that collide with a surface molecule and, in turn, the probability that the same molecule will be liberated from the surface.²¹ Self-assembled monolayers are well-ordered arrays of individual organic molecules attached to Au surfaces through single Au–S bonds. The exchanged targets used in our experiments consist of anions ionically bound to the end of a short-chain thiol presumably standing "on end" with respect to the Au substrate. We assume, due to the mass and energy of the projectile atoms used in this study, that the recoil collision cascades are generated predominantly within the 200 nm Au substrate layer. It is unlikely that two or more individual recoil cascades generated within the Au substrate by constituents of the same polyatomic ion will intersect at the same Au surface atom to eject the bound

anion. It is also unlikely that multiple "hits" to the same monolayer molecule are necessary to liberate adsorbed BF_4^- or B(Ph)_4^- due to the weak electrostatic interaction we assume holds the anion to the protonated amine terminus. If we assume that the recoil cascades generated by each projectile constituent independently intersect the surface to eject an adsorbed anion, then the relative anion yield should scale linearly with the number of projectile atoms. This hypothesis is supported by the ion yield measurements conducted in the present study.

Two recent studies focused on the comparison of atomic and polyatomic ion impacts on ultrathin films. Hanley and co-workers compared ion yields from a target surface composed of NH_3 physisorbed to a CO monolayer on Ni.¹¹ In their study, SF_5^+ projectiles produced higher yields of NH_3 relative to the area of surface damaged when compared to Xe^+ at impact energies < 1 keV. At the low incidence energies employed, where direct knock-on sputtering predominates, the enhancement produced by the SF_5^+ primary ion was attributed to the reflection of the projectile atoms by the Ni surface. In a more recent study, Stapel et al. demonstrated that the yield enhancement produced by SF_5^+ projectiles (over Ar^+ and Xe^+ projectiles at equal impact energy) on a single Langmuir–Blodgett (LB) layer is significantly lower when compared to multilayer LB films.¹² The results of the present study demonstrate that similar behavior is exhibited when polyatomic ions are used to bombard anion-exchanged self-assembled monolayer surfaces.

Molecular dynamics (MD) methods have been used to simulate the Cu atomic and Cu_n cluster projectile impacts on surfaces consisting of a monolayer of biphenyl molecules on Cu. It is interesting to note that as a consequence of the study, Krantzman and co-workers predicted that the yield of intact molecules from the surface will increase linearly with the number of incident atoms when compared at the same projectile energy per atom.²³ Our experimental results, though using a different model system, qualitatively confirm the predictions based on the MD simulations.

Conclusions

To our knowledge, this is the first demonstration of the adsorption of complex inorganic anions to the surface of an amine-terminated self-assembled monolayer with subsequent measurements of ion yields from energetic ion bombardment. The uptake of BF_4^- and B(Ph)_4^- by various prepared surfaces was monitored using SIMS with Cs^+ ion bombardment. By comparing AET, propanethiol, and Au on Si surfaces, we have demonstrated that the positively charged amine terminus of the AET monolayer promotes the anion adsorption. The adsorption is reversible, and recent experiments have shown that a single monolayer surface can be used repeatedly for exchange studies.²⁴

We have also shown that the secondary ion yield trend, *per projectile constituent*, is markedly different when comparing the bombardment of anion-exchanged monolayer and thick solid target surfaces by keV energy atomic and polyatomic ion projectiles. The polyatomic projectiles produced nonlinear yield enhancements from the thick targets. The anion yields from the exchanged surfaces scale nearly linearly with the number of projectile constituents. A slight enhancement using $(\text{CsI})\text{Cs}^+$ over Cs^+ and $(\text{CsI})_2\text{Cs}^+$ was observed. This enhancement, however, was greatly reduced compared to sputtering from the thick targets. The difference in the yield enhancement trends is influenced the most by the unusually high ion yields generated by Cs^+ impacts on the exchanged monolayers. Our experiments indicate that for the analysis of exchanged monolayer surfaces only small improvements in the efficiency of ion production is gained by using a polyatomic primary ion.

The uptake and exchange of ions to the amine-terminated self-assembled monolayers represents a potentially new and effective way to concentrate negatively charged analyte molecules from solution for subsequent analysis by TOF-SIMS. For instance, cationic surfactants are known to improve the yield of inorganic anions in negative ion SIMS.^{25,26} In a similar approach, McNeal and Macfarlane used Mylar films impregnated with cationic surfactants to exchange anions from solution for mass analysis using plasma desorption mass spectrometry.²⁷ More recently, Orlando and co-workers described a protocol for desalting analyte solutions for MALDI mass analysis, exploiting the ion-pair formation induced by the protonated amine terminus.¹⁶

Acknowledgment. The authors would like to acknowledge W. Baker and R. M. Crooks for technical assistance with the growth of self-assembled monolayer surfaces and supplying the aminoethane thiol. This work was supported by the National Science Foundation (Grant CHE-9727474).

References and Notes

- (1) Van Stipdonk, M. J.; Harris, R. D.; Schweikert, E. A. *Rapid Commun. Mass Spectrom.* **1996**, *10*, 1987.
- (2) Harris, R. D.; Van Stipdonk, M. J.; Schweikert, E. A. *Int. J. Mass Spectrom. Ion Processes* **1998**, *174*, 167.
- (3) Benguerba, M.; Brunelle, A.; Della-Negra, S.; Depauw, J.; Joret, H.; Le Beyec, Y.; Blain, M. G.; Schweikert, E. A.; Ben Assayag, G.; Sudraud, P. *Nucl. Instrum. Methods B* **1991**, *62*, 8.
- (4) Appelhans, A. D.; Delmore, J. D. *Anal. Chem.* **1989**, *61*, 1087.
- (5) Groenewold, G. S.; Delmore, J. E.; Olson, J. E.; Appelhans, A. D.; Ingram J. C.; Dahl, D. A. *Int. J. Mass Spectrom. Ion Processes* **1997**, *163*, 185.
- (6) Hand, O. W.; Majumdar, T. K.; Cooks, R. G. *Int. J. Mass Spectrom. Ion Processes* **1990**, *97*, 35.
- (7) Szymczak, W.; Wittmaack, K. *Nucl. Instrum. Methods* **1994**, *B88*, 149.
- (8) Roberson, S.; Gillen, G. *Rapid Commun. Mass Spectrom.* **1998**, *12*, 1303.
- (9) Kötter, F.; Niehuis, E.; Benninghoven, A. in *Secondary Ion Mass Spectrometry, SIMS XI*; Gillen, G., Lareau, R., Bennett, J., Stevie, F., Eds.; John Wiley & Sons: New York, 1998; p 459.
- (10) Kötter, F.; Benninghoven, A. *Appl. Surf. Sci.* **1998**, *133*, 47.
- (11) Ada, E. T.; Hanley, L. *Int. J. Mass Spectrom. Ion Processes* **1998**, *174*, 231.
- (12) Stapel, D.; Brox, O.; Benninghoven, A. *Appl. Surf. Sci.* **1999**, *140*, 156.
- (13) Harris, R. D.; Baker, W. M.; Van Stipdonk, M. J.; Crooks, R. D.; Schweikert, E. A. *Rapid Commun. Mass Spectrom.*, accepted for publication.
- (14) Nuzzo, R. G.; Zegarski, B. R.; Dubois, L. H. *J. Am. Chem. Soc.* **1987**, *109*, 733.
- (15) Patrick, J. S.; Cooks, R. G.; Pachuta, S. J. *Biol. Mass Spectrom.* **1994**, *23*, 653.
- (16) Warren, M. E.; Brockman, A. H.; Orlando, R. *Anal. Chem.* **1998**, *70*, 3757.
- (17) Tarlov, M. J.; Newman, J. G. *Langmuir* **1992**, *8*, 1398.
- (18) The monolayers were oxidized for 15 min using a Hg/Ar spectral calibration lamp (Oreil). The distance from the UV source to the monolayer surface was 4 cm, providing a photon dose of $\sim 1 \mu\text{W}/\text{cm}^2$.
- (19) Van Stipdonk, M. J.; Justes, D. R.; Santiago, V.; Schweikert, E. A. *Rapid Commun. Mass Spectrom.* **1998**, *12*, 1639.
- (20) Blain, M. G.; Della-Negra, S.; Joret, H.; Le Beyec, Y.; Schweikert, E. A. *Phys. Rev. Lett.* **1989**, *63*, 1625.
- (21) Van Stipdonk, M. J.; Santiago, V.; Schweikert, E. A. *J. Mass Spectrom.*, accepted for publication.
- (22) Žarić, R.; Pearson, B.; Krantzman, K. D.; Garrison, B. J. In *Secondary Ion Mass Spectrometry, SIMS XI*; Gillen, G., Lareau, R., Bennett, J., Stevie, F., Eds.; J. Wiley and Sons: Chichester, 1998; p 601.
- (23) Townes, J. A.; White, A. K.; Krantzman, K. D.; Garrison, B. J. *Proceedings of the Fifteenth International Conference on the Application of Accelerators in Research and Industry*, in press.
- (24) Van Stipdonk, M. J. Unpublished results.
- (25) Ligon, W. V., Jr.; Dorn, S. B. *Int. J. Mass Spectrom. Ion Processes* **1985**, *63* (2–3), 315.
- (26) Ligon, W. V., Jr.; Dorn, S. B. *Int. J. Mass Spectrom. Ion Processes* **1986**, *68* (3), 337.
- (27) McNeal, C. J.; Macfarlane, R. D. *J. Am. Chem. Soc.* **1986**, *108* (9), 2132.